Atmospheric Pollution Research 9 (2018) 146–155

HOSTED BY

Contents lists available at ScienceDirect

Atmospheric Pollution Research

journal homepage: http://www.journals.elsevier.com/locate/apr



Chemical analysis of particulate products of aged 1,3,5-trimethylbenzene secondary organic aerosol in the presence of ammonia

Mingqiang Huang [a, b, *], Jun Xu [a], Shunyou Cai [a], Xingqiang Liu [b], Changjin Hu [c], Xuejun Gu [c], Weixiong Zhao [c], Li Fang [c], Weijun Zhang [c, **]

[a] Fujian Provincial Key Laboratory of Modern Analytical Science and Separation Technology, College of Chemistry & Environment, Minnan Normal University, Zhangzhou, 363000, China
[b] College of Environmental Science and Engineering, Xiamen University, Tan Kah Kee College, Zhangzhou, 363105, China
[c] Laboratory of Atmospheric Physico-Chemistry, Anhui Institute of Optics and Fine Mechanics, Chinese Academy of Sciences, Hefei, 230031, China

ARTICLE INFO

Article history:
Received 7 June 2017
Received in revised form
20 August 2017
Accepted 20 August 2017
Available online 26 August 2017

Keywords:
1,3,5-Trimethylbenzene
Secondary organic aerosol
Ammonia
Brown carbon
Aging mechanisms

ABSTRACT

Ammonia (NH_3) gas-aging of secondary organic aerosol (SOA) results in the formation of organonitrogen compound is an important class of brown carbon. The particulate products of aged 1,3,5-trimethylbenzene (135-TMB) SOA in the presence of NH_3 were measured by UV–Vis spectrophotometer, attenuated total reflectance-Fourier transform infrared (ATR-FTIR), and aerosol laser time-of-flight mass spectrometer (ALTOFMS) in present study. Experimental results indicated that NH_3 has significant promotion effect on 135-TMB SOA formation. Organic ammonium salts, such as ammonium methyl glyoxylate, ammonium 3,5-dimethylbenzoate, which are formed from NH_3 reactions with gaseous organic acids were detected as the principal particulate products of NH_3-aged 135-TMB SOA. 4-methyl-imidazole-2-acetaldehyde, 4-methyl- 1H-imidazole and other imidazole products via the heterogeneous reactions between NH_3 and dialdehydes of 135-TMB SOA were newly measured. The formation of imidazole products suggests that some ambient particles contained organonitrogen compounds may be come from this mechanism. The results of this study may provide valuable information for discussing SOA aging mechanisms and new route for NH_3 deposition.

© 2017 Turkish National Committee for Air Pollution Research and Control. Production and hosting by Elsevier B.V. All rights reserved.

1. Introduction

1,3,5-trimethylbenzene (135-TMB) and other aromatic hydrocarbons emitted from motor vehicles are main precursors of secondary organic aerosol (SOA) formation (Ziemann and Atkinson, 2012; Li et al., 2016; Gentner et al., 2017). SOA particles in the atmosphere can have lifetime of about one week (Rudich et al., 2007; Andreae, 2009), during which they can age via reaction with nitrogen oxides (NO_x), ammonia (NH_3) and other reduced nitrogen species, leading to the formation of organonitrogen compounds of brown carbon (Updyke et al., 2012; Flores et al., 2014; Lin et al., 2015; Liu et al., 2015), which absorb radiation efficiently in the near-UV (300–400 nm) and short wavelengths of visible ranges (Laskin et al., 2015), and have a vital contributor to radiative forcing (Andreae and Ramanathan, 2013; Laskin et al., 2015; Tang et al., 2016).

Ammonia (NH_3) from livestock waste, fertilizers, gasoline vehicles and other non-agricultural sources is the primary alkaline pollution gas commonly found in the atmosphere (Paulot et al., 2014; Sun et al., 2017). Recently, it has been shown that NH_3 plays an important role in the aging of SOA particles. SOA particles formed from the OH- and O_3-initiated oxidation of anthropogenic and biogenic precursors were exposed to NH_3 were performed by Updyke et al. (2012), the measured highest mass absorption coefficients (MAC) of SOA from limonene and

* Corresponding author. Fujian Provincial Key Laboratory of Modern Analytical Science and Separation Technology, College of Chemistry & Environment, Minnan Normal University, Zhangzhou, 363000, China.
** Corresponding author.
E-mail addresses: huangmingqiang@gmail.com (M. Huang), wjzhang@aiofm.ac.cn (W. Zhang).

Peer review under responsibility of Turkish National Committee for Air Pollution Research and Control.

http://dx.doi.org/10.1016/j.apr.2017.08.003
1309-1042/© 2017 Turkish National Committee for Air Pollution Research and Control. Production and hosting by Elsevier B.V. All rights reserved.

sesquiterpenes ozonolysis, were matched up to MAC values of biomass burning particles. The complex refractive indices (RI) of brown carbon from biogenic SOA aged with NH_3 were measured by Flores et al. (2014) with broadband cavity enhanced spectroscopy. The obtained real component (n) of the NH_3-aged biogenic SOA did not change significantly, but the imaginary part (k) increased from k = 0.000 to 0.030 for the NH_3-aged limonene and α-humulene SOA. Also, the particulate nitrogen-containing organic products formation during the photooxidation of m-xylene and ozonolysis of α-pinene with NH_3 were studied by Liu et al. (2015). A number of organonitrogen fragments were observed which were in accordance with the reactions between NH_3 and carbonyl constituents of SOA.

The above experiments mainly focused on the measurement of optical parameters (MAC, RI) of the NH_3-aged biogenic SOA. However, the detail chemical constituents of organonitrogen products of brown carbon were not considered in these reports. Recently, our group has used aerosol laser time-of-flight mass spectrometer (ALTOFMS) coupled with Fuzzy C-Means (FCM) clustering algorithm to measure the chemical compositions of aged 135-TMB SOA with or without inorganic aerosol seeds successfully (Huang et al., 2015, 2017). On this basis, the effect of NH_3 on the formation and aging of SOA formed from photooxidation of 135-TMB were explored in the present study, and the chemical constituents of particulate products were measured with UV–Vis spectrophotometer, attenuated total reflectance-Fourier transform infrared (ATR-FTIR) and ALTOFMS, respectively. Reaction mechanisms leading to organonitrogen products of brown carbon were also discussed.

2. Experimental method

2.1. 135-TMB SOA formation and aging in the presence of NH_3

135-TMB (>99%) was bought from Sigma-Aldrich Chemistry Corporation, Germany. NO (99.9%) and NH_3 (99.9%) were provided by Special Gas Factory of Nanjing. CH_3OH (>99%), H_2SO_4 (98%) and $NaNO_2$ (>99%) were obtained from Third Reagent Manufactory of Tianjin. CH_3ONO was synthesized by dropping H_2SO_4 with a solution of $NaNO_2$ dissolved in CH_3OH and was used after vacuum distillation to remove any CH_3OH, NO_x and other impurities (Huang et al., 2015).

Formation and aging of 135-TMB SOA were performed in the 850 L smog chamber equipped with black lamps (the radiation wavelength in range of 300–400 nm, and peak intensity at 365 nm, the rate constant of NO_2 photolysis is $0.21 \pm 0.01\ min^{-1}$) similarly to the procedure described by our published studies (Huang et al., 2015, 2017). In total eight experiments were designed with NH_3 present or absent under the conditions listed in Table 1. In all experiments, the temperature and relative humidity in chamber was maintained at about 300 ± 2 K and 25 ± 2%, respectively. OH radicals are formed from the irradiation of methyl nitrite using 4 black lamps (Atkinson et al., 1981). GC-FID (Agilent 7820A), NO-NO_2-NO_x analyzer (TEI model 42i), a home-built ultraviolet–visible spectroscopy of Chernin cell system, O_3 analyzer (TEI model 49i), NH_3 analyzer (TEI model 17i) and SMPS (TSI 3080L DMA, TSI 3775 CPC) was used to measure the concentrations of 135-TMB, NO_x, CH_3ONO, O_3, NH_3 and the mass concentrations of SOA particles every 30 min, respectively. Each experiment was repeated 3 times in parallel, twice for collecting aged particles for off-line analysis with UV–Vis spectrophotometer and ATR-FTIR after 24 h photooxidation, and the other for online analysis with ALTOFMS coupled with FCM clustering algorithm.

2.2. UV–Vis and infrared spectroscopy of aged 135-TMB SOA

After 24 h photooxidation, the aged 135-TMB SOA particles were collected onto polytetra fluoroethylene membrane filters (Sigma-Aldrich Chemistry Corporation, 47 mm, 0.20 μm pore size) at 3 L/min for 2 h. The constituents of the filtered aged particles were extracted into 5 mL of 2% methanol water solution (2% methanol in volume) using 30 min sonication for off-line measurements. A double beam UV–Vis spectrophotometer (UV-6100S, Mapada Instruments) was used to measure the absorbance of the extracts from 200 to 600 nm. The spectrophotometer was blanked using a 1 cm quartz cuvette filled with 2% methanol water solution. Since the extracts are the solution samples, they cannot be measured by the conventional infrared spectrometer equipped with a KBr beamsplitter. The infrared spectra of extracts were recorded on an ATR-FTIR (Thermo Nicolet iS 10, Thermo Fisher Scientific) equipped with DTGS detector, which can be used for determination of solution samples directly. ATR-FTIR was performed in autogain mode, and data was obtained between 4000 and 400 cm^{-1} with the resolution of 2 cm^{-1}. In an effort to verify the formation of aged products, the reference absorption spectrum of blank sample formed from extraction of polytetra fluoroethylene membrane filter in 5 mL of 2% methanol water solution using 30 min sonication was taken prior to any 135-TMB SOA filter extract analysis.

2.3. Mass spectra of aged 135-TMB SOA

The aged SOA particles are measured by ALTOFMS coupled with FCM clustering algorithm in real-time. The aged SOA particles were transferred into the ALTOFMS via the aerodynamic lens and entered to the sizing system for velocity/size determination and chemical component analyzing system sequentially. The particles with successfully measured diameters were ionized by the pulsed KrF excimer laser. The formed ions were analyzed in a linear time-of-flight mass spectrometer. The acquired mass spectra of particles were calibrated with well-known ions for the recorded mass spectra and converted to a normalized 300-point vector. The data vectors of all particles measured were written into a classification matrix. Each spectrum's data was stored as one row in this matrix.

Table 1
Initial experimental conditions of the formation and aging of 135-TMB SOA.

Run Number	[135-TMB] (ppm)	[NO] (ppm)	[CH_3ONO] (ppm)	[NH_3] (ppm)	Temperature (K)	RH (%)
1	2.0	2.1	20.2	0.0	301	24
2	1.9	2.0	20.0	2.2	299	26
3	2.2	2.1	20.1	4.1	300	25
4	2.0	2.2	19.9	8.3	298	27
5	1.9	2.0	20.1	12.2	302	26
6	2.1	2.0	19.8	16.1	300	25
7	2.0	2.2	20.2	20.3	298	27
8	0.0	2.0	20.1	20.2	300	25

Then, the mass spectra of individual particles were further handled by FCM algorithm (Huang et al., 2015, 2017).

FCM algorithm is an iterative method that starts the calculation with random class centers to find a substructure in the data. It calculates a fuzzy partition matrix to determine d_{ik} of the distance between data vector i and each class center k, and to group i into k cluster via the minimum value of d_{ik}. FCM works in such a way that the cluster number of similar objects and each class center could be determined. Each class center represented as a "mean" mass spectra pattern, which was used for the characterization of the constituents of the particle class. Davies-Bouldin (DB) index was utilized to evaluate the optimum cluster number among different partitions. It is defined as:

$$DB = \frac{1}{n}\sum_{i=1,j\neq i}^{n} \max\left\{\frac{\sigma_i + \sigma_j}{d(c_i, c_j)}\right\}$$

where n is the number of clusters, σ_i and σ_j is the average distance of all patterns in cluster i and j to their respective cluster center c_i and c_j, respectively, and $d(c_i,c_j)$ is the distance of cluster centers c_i and c_j. Small values of DB correspond to clusters that are compact, and whose centers are far away from each other. So, the number of clusters that minimizes DB is taken as the optimal number of clusters (Huang et al., 2015, 2017).

3. Results and discussions

3.1. Effect of NH_3 on 135-TMB SOA formation

It is well known that NO_2 could be oxidized by the reaction with OH radicals to form nitric acid (Atkinson et al., 2004). Nitric acid will react with NH_3 in gas phase or on particle surface to produce ammonium nitrate particles, which may contribute to the formation of secondary aerosol particles in smog chamber. However, it is worth noting that NO was added in the current experimental condition. According to the kinetic and photochemical data proposed by Atkinson et al. (2004), the rate coefficient for $2NO + O_2 \rightarrow 2NO_2$ is 2.0×10^{-38} cm^6 $molecule^{-2}$ s^{-1} at 298 K, indicating that very few NO_2 may existed in smog chamber. Also, part of NO_2 could be photolysis by the radiation of black lamps. The control experiment (Run 8) was performed to verify whether the ammonium nitrate particles derived from NO_2, OH radicals and NH_3 are present in the chamber. The mass concentration of aerosol particle is measured by SMPS and corrected for wall loss (Huang et al., 2013). The measured mass concentration of particle in smog chamber is less than 0.1 $\mu g/m^3$ during 24 h photooxidation with 4 black lamps for Run 8. In addition, no mass spectrum was obtained by ALTOFMS after 24 h photooxidation for the control experiment. These results demonstrating that there was nearly no ammonium nitrate particles formation in the photooxidation of CH_3ONO, NO and NH_3, and ammonium nitrate particles formed from NO_2, OH radicals and NH_3 have scarcely contribution to the formation of secondary aerosol particles in the present reaction system.

The effect of NH_3 on the formation of 135-TMB SOA was examined by comparing SOA growth in different concentrations of NH_3 as listed in Table 1. SOA growth is defined as plotting the mass concentration of 135-TMB SOA as a function of reaction time. As shown in Fig. 1, the corrected maximum mass concentration of 135-TMB SOA in the presence of NH_3 is in the range of 145–208 $\mu g\ m^{-3}$, larger than that measured for the experiment without NH_3 of 122 $\mu g\ m^{-3}$, indicating that NH_3 has significant promotion influence on 135-TMB SOA formation. The formed mass concentration of 135-TMB SOA increases by 19% to 70% as the added NH_3 increases from 2.2 to 20.3 ppm. The results consist of the findings reported by Na et al. (2007), as they considered that NH_3 promotes gaseous organic acids formed from O_3-initiated oxidation of α-pinene into particulate organics, leading to the formation of organic ammonium salts and elevated mass concentrations of SOA. It is worth noting that no additional aerosol formation when the added NH_3 exceeds 16 ppm.

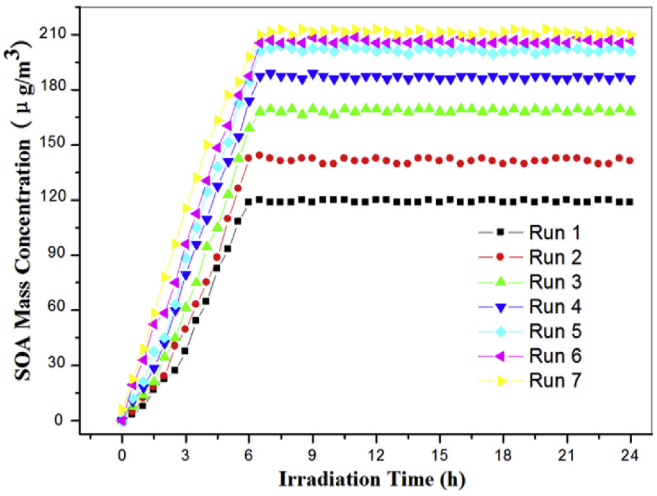


Fig. 1. Corrected 135-TMB SOA mass concentration (average for the 3 repeated experiments) measured as a function of irradiation time for Run 1–7.

It also can be seen from Fig. 1 that the 135-TMB SOA mass concentration reaches the maximum at about 6 h, SOA aging occur for another 18 h afterwards. Before 6 h in this study, there were plenty of 135–TMB and OH radicals to generate SOA particles, where we observed the mass increase. While afterward, there was not 135-TMB available to react with OH radicals to produce new particles, SOA aging processes occur via semivolatile products in the gas phase continue to react with OH radicals and NH_3 or SOA particles heterogeneous uptake of OH radicals and NH_3 under UV illumination. OH-initiated oxidation of semivolatile precursors in the gas phase may result in less volatile and more hydrophilic products, and thus may enhance the mass concentration of SOA. Also, SOA particles heterogeneous uptake of NH_3 can increase SOA mass by converting gaseous NH_3 into SOA as organonitrogen compounds. On the other hand, as SOA particles containing oxygenated organics, according to the experimental results of Kroll et al. (2009) and George and Abbatt (2010), the fragmentation mechanism becomes the dominant oxidation mechanism for the OH-initiated heterogeneous oxidation of oxidized organic aerosol. OH-initiated heterogeneous oxidation of SOA particles may decrease SOA mass due to volatilization of oxidation products. Therefore, these complex aging processes may result in a slightly increase or decrease in the mass concentration of SOA in the smog chamber. However, the aged SOA particles can also deposited onto the chamber wall causing the aerosol losses. The smog chamber used in the current study has the large wall loss rate owing to its small volume, about 70–80% of aged SOA particles deposited on the chamber wall after 24 h photooxidation (Huang et al., 2015, 2017). Thus, the wall loss is the main factor in reducing the mass concentration of SOA in the present experiments. Compared to wall loss, the aging processes lead to a slightly increase or decrease in the mass concentration of SOA is almost negligible. So, the mass concentration of SOA during the 18 h aging period was almost constant after correcting for wall loss as shown in Fig. 1. The SOA particles in smog chamber are the aged SOA particles after 24 h photooxidation.

3.2. UV–Vis and IR spectra of aged 135-TMB SOA

The absorption spectrum of blank sample formed from extraction of polytetra fluoroethylene membrane filter in 5 mL of 2% methanol water solution using 30 min sonication was check firstly. Either the UV–Vis or IR spectra of blank sample exhibits any detectable optical absorption around 200–600 nm or 4000-400 cm^{-1}, demonstrating that no additional organic material in the extraction solution of polytetra fluoroethylene membrane filter. Fig. 2 displays the typical UV–Vis spectra of the aged 135-TMB SOA extracts for the Run 1 and Run 7. From the UV–Vis spectra over the range of 200–600 nm, we can observe that aged 135-TMB SOA particles absorb light at wavelengths <300 nm but have negligible absorption in the visible range (300–600 nm). Our results are consistent with Li et al. (2014) and Nakayama et al. (2013), who have studied the optical properties of SOA particles from photooxidation of aromatic compounds and have found that 135-TMB SOA particles have no obvious absorption in the visible range. However, the UV–Vis spectrum of aged 135-TMB SOA without NH_3 (Run 1) has a distinctive absorption signal at 205 nm. This spectral characteristic matches the light absorption property of carboxyl compound (Carlton et al., 2007), indicating that carboxyl compounds are the major constituents of aged 135-TMB SOA particles without NH_3. In fact, carboxylic acids, such as 3,5-dimethylbenzoic acid, methyl glyoxylic acid, 2-methyl-4-oxo-2-pentenoic acid, have already measured as major products in aged 135-TMB SOA (Huang et al., 2015). Also, carboxylic acids were further confirmed by the infrared spectra of the SOA filter extract for Run 1 illustrated in Fig. 3(a). The broad peak near 3255 cm^{-1} and 1643 cm^{-1} was assigned to O-H and unconjugated C=O stretching of carboxyl groups, respectively. The peak at 1055 cm^{-1} could be attributed to O-H bending vibrations and C-O stretching of carboxyl groups (Chang and Thompson, 2010). These peaks beg the conclusion that major products of aged 135-TMB SOA particles without NH_3 are carboxylic acids.

Besides to the absorption band at 205 nm, there is an additional absorption signal at 280 nm in the UV–Vis spectra of aged 135-TMB SOA with NH_3 (Run 7). It can be seen from Fig. 2 that the intensity of 205 nm absorption peak in the UV–Vis spectrum of Run 7 is stronger than that of Run 1, indicating that the content of carboxyl compounds of aged 135-TMB SOA with NH_3 is higher than that of aged SOA without NH_3. This result provides further testimony that NH_3 can react with gaseous organic acids generating carboxylates as suggested by Na et al. (2007). The newly emerging of absorption peak of 280 nm indicates that the formation of new products in aged SOA with NH_3. This band was also observed in evaporating droplets containing glyoxal and $(NH_4)_2SO_4$ conducted by Lee et al. (2013) and in previous bulk studies (Kampf et al., 2012; Maxut et al., 2015) using solute concentrations of glyoxal and $(NH_4)_2SO_4$ in molar level. The potential chromophores were likely imidazole compounds, such as 4-methyl-1H-imidazole, 4-methyl-imidazole-2-acetaldehyde which were formed from the reactions between NH_3 and carbonyl-containing SOA. Although carboxyl compounds, whose IR absorbance bands shown in Fig. 3(b) (for Run 7) appear at 1649 cm^{-1} for the stretching of C=O, 1087 cm^{-1} for the bending vibration of O-H and stretching of C-O were observed, the notable peaks appear at 1518 cm^{-1} for bending of N-H, 1743-1698 cm^{-1} for stretching of N=C, and 1457 cm^{-1} for stretching of C-N (Liu et al., 2015), confirming that the 280 nm chromophores correspond to imidazole compounds. Also, the observed ALTOFMS fragments of CH_2N^+ (m/z 28), $C_2H_3N^+$ (m/z 41) and $C_3H_3N_2^+$ (m/z 67) in the next section indicates imidazole compounds have formed in the aged 135-TMB SOA with NH_3.

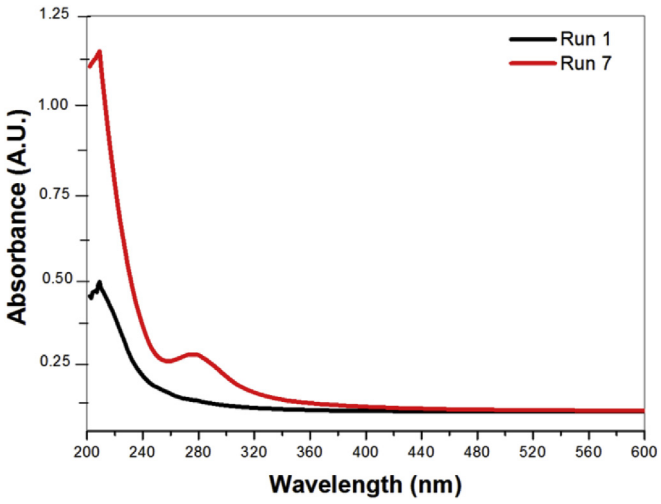


Fig. 2. UV–Vis spectra of the 135-TMB SOA filter extract for Run 1 and Run 7.

3.3. Mass spectra of aged 135-TMB SOA

The aged 135-TMB SOA particle which has similar mass spectra could be clustered into the same class by FCM algorithm. As the aged SOA particles formed from the photooxidation of aromatic compound is a complex mixture. Particle class obtained by FCM may contain one or more components. However, it is difficult to obtain all the chemical components of the aged particle class with its mass spectrum. Generally, the high content of the component (major constituent) whose mass peaks in the mass spectrum of particle class have high intensity, and the peak intensity of the mass spectrum are small for the less abundant components. The major chemical constituent of the particle class was speculated by references to the corresponding reaction and aging mechanisms of OH-initiated photooxidation of aromatic compounds and the comparisons with the characteristic cleavage fragment peaks of the mass spectra pattern of the particle class. Then, the major mass peaks of particle class were compared and validated in detail with the mass spectra of commercial chemical compounds measured by ALTOFMS or the available mass spectra of the aged products found in the NIST database. The mass peaks of minor constituent with low intensity were not analyzed, and each particle class was considered corresponding to a major aging product (Huang et al., 2015, 2017).

The particulate products of aged 135-TMB SOA in the absence of NH_3 have already measured by ALTOFMS coupled with FCM algorithm in our previous study (Huang et al., 2015). In addition to the high-molecular-weight (HMW) components of Class 10–12, the mass spectra of the clusters of aged 135-TMB SOA without NH_3 (Run 1) contained the fragment peaks m/z 44 (CO_2^+) and 46 (NO_2^+), demonstrating that these clusters attribute to the caroboxylic acid (methyl glyoxylic acid, 2-methyl-4-oxo-2-pentenoic acid, 3,5-dimethylbenzoic acid, 2-methyl-2,3-dihydroxyl-4-oxo-pentanoic acid, 3,4-dimethyl-2-hydroxy-3-oxo-pentandioic acid, 2,4-dimethyl-2,3-dihydroxy-6-oxo-4-heptenoic acid, 2,4-dimethyl-4-hydroxyl-2,3-epoxy-heptylic acid, 2,4-dimethyl-2,3,4-trihydroxy-5,6-dioxo-heptylic acid) and dimethylnitrophenol (3,5-dimethyl-2-nitrophenol, 3,5-dimethyl-4-nitrophenol) compounds, respectively.

About 6500 pieces of single particle mass spectra of Run 7 were selected to extract out potential aerosol with FCM algorithm. The Davies–Bouldin index shown in Fig. 4 has the minimum value at n = 14, indicating that the aged SOA particles of Run 7 can be clustered into 14 classes. It can be seen from Fig. 5 that the ion signal of m/z 18 (NH_4^+) and m/z 44 (CO_2^+) were found in the mass

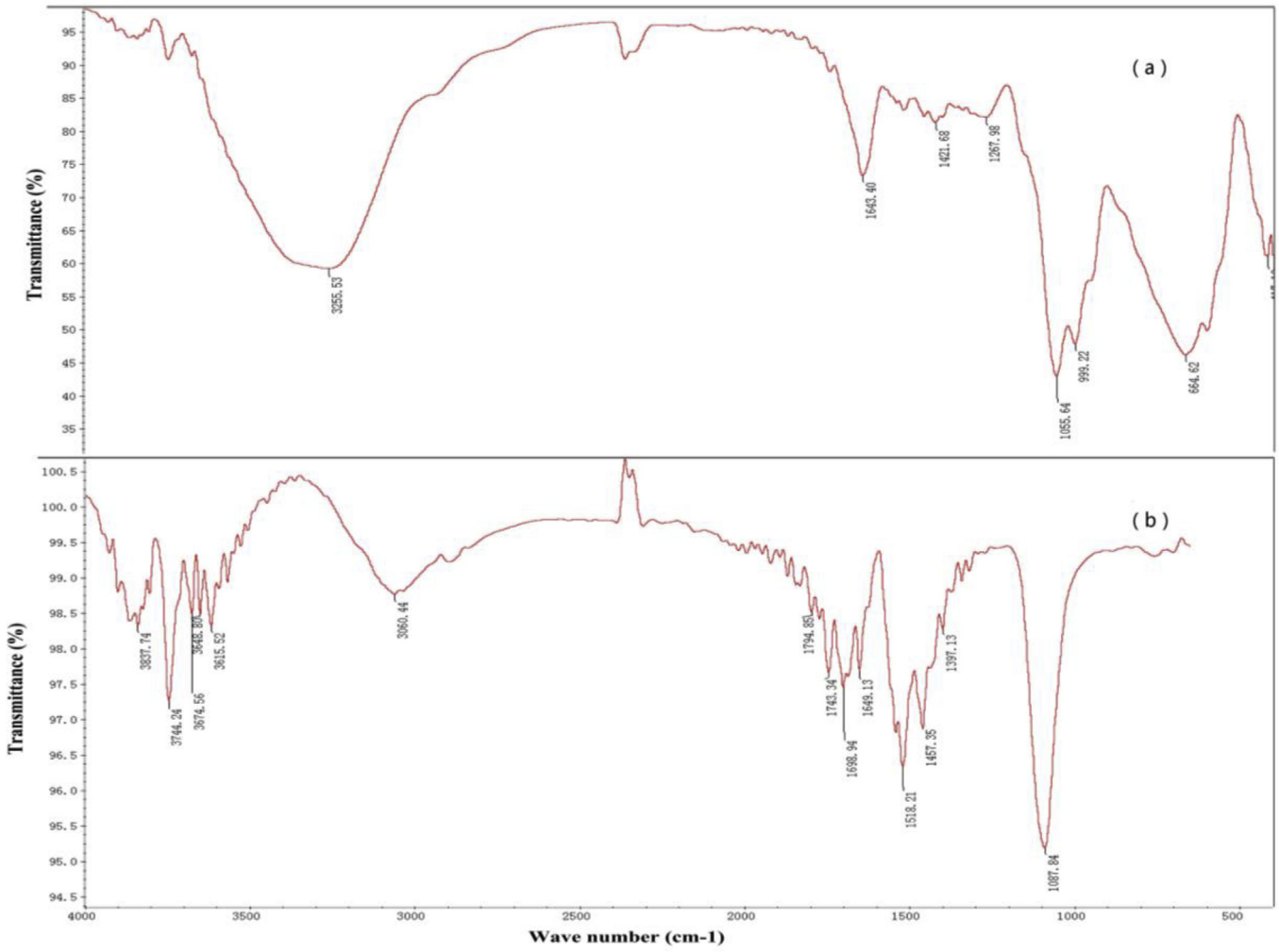


Fig. 3. Infrared spectra of the 135-TMB SOA filter extract for (a) Run 1 and (b) Run 7.

spectral pattern of Class 1–8 of aged 135-TMB SOA in the presence of NH_3 (Run 7), demonstrating that organic ammonium carboxylates are the predominant products in the 135-TMB SOA aged with NH_3. To validate identification of the ammonium carboxylates, two pure chemical compounds of ammonium formate and ammonium oxalate were dissolved in 2-propanol (about 1×10^{-5} g ml^{-1} for each compound) and atomized by a constant output atomizer (TSI Inc. Model 3076), then subsequently passed through a diffusion dryer (TSI Inc. Model 3062, USA), an ^{85}Kr charge neutralizer (TSI Inc., Model 3054, USA) before entering ALTOFMS for detection. The average mass spectrum out of 100 spectra for particles of each commercial reference compound is shown in Supplementary Fig. S1. Besides to the characteristic fragment peaks of ammonium carboxylates at m/z 18 (NH_4^+) and m/z 44 (CO_2^+), the molecular ion of ammonium formate and ammonium oxalate was observed at m/z 63 ($HCOONH_4^+$) and m/z 124 ($(NH_4)_2C_2O_4^+$) in their mass spectra displayed in Supplementary Fig. S1. These results are consistent with Silva and Prather (2000), who have analyzed organic compounds include organic salts using aerosol time-of-flight mass spectrometry, and protonated molecular ion was detected in the laser desorption/ionization mass spectra of organic ammonium salt. The mass spectra patterns of Class 1 to Class 8 are similar to the mass spectra of ammonium formate and ammonium oxalate, which gave us confidence to speculate the Class 1 to Class 8 as organic ammonium carboxylates. 3,5-dimethyl-benzaldehyde, methylglyoxal, 2,4-dimethyl-2-pentendial, 2-methyl-4-oxo-2-pentenal, 2,4-dimethyl-6-oxo-2,4-heptadiene, 2,4-dimethyl-2,3-epoxy-6-oxo-4-heptene which are the major gaseous aldehydes

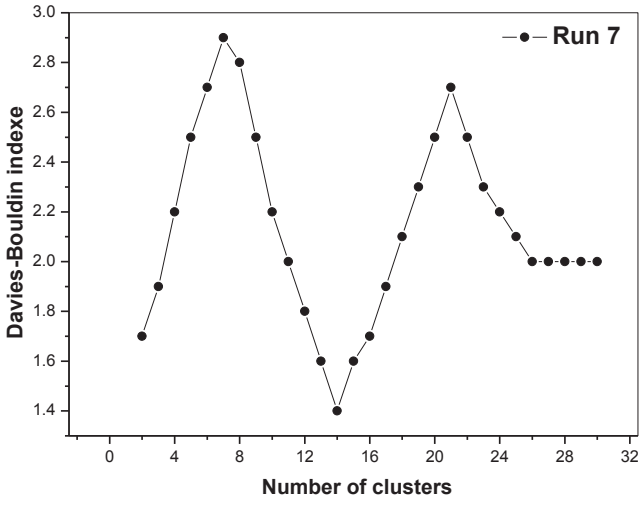


Fig. 4. Clustering number evaluated using the Davies–Bouldin index for the aged 135-TMB SOA particles in the presence of NH_3 of Run7.

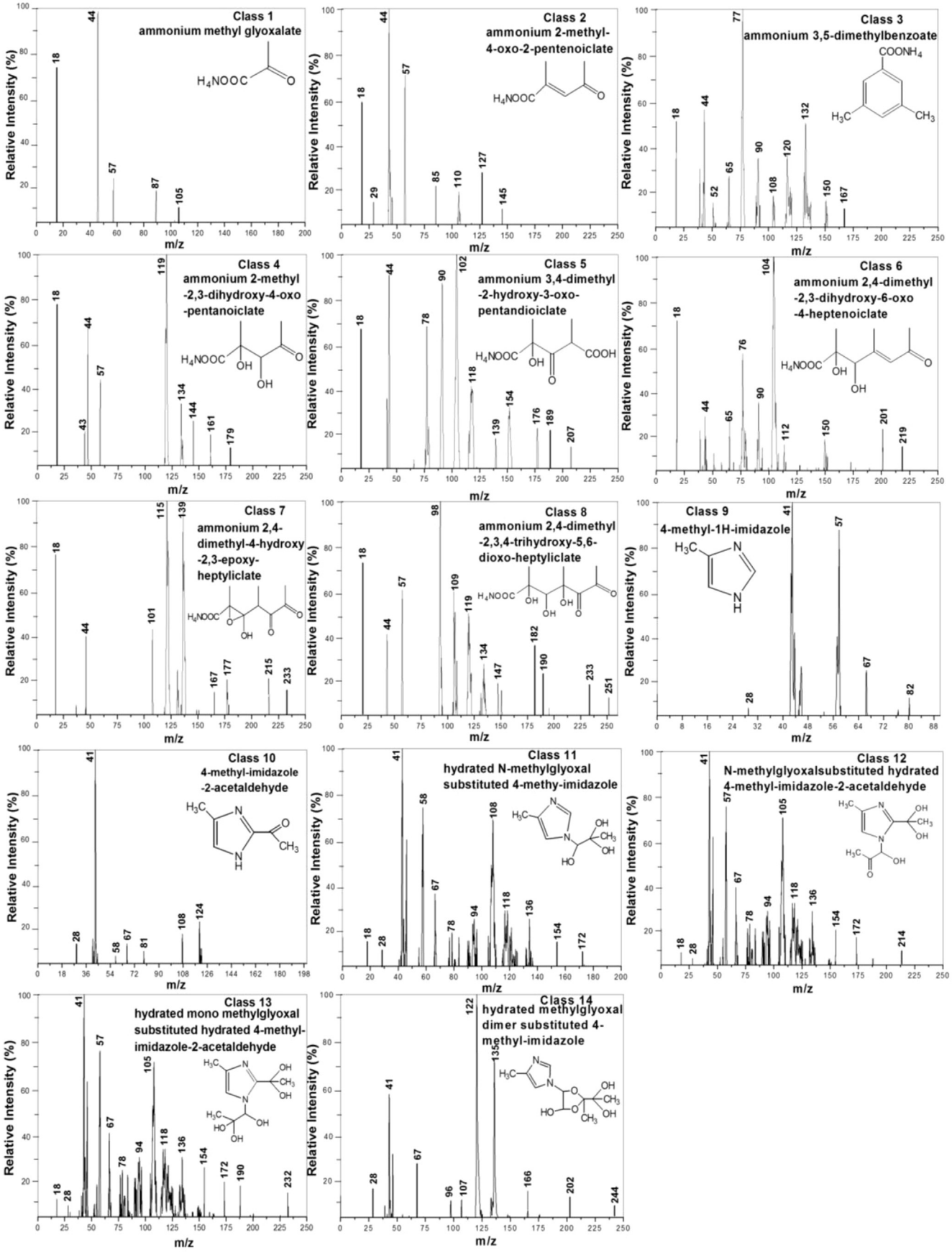


Fig. 5. Representative spectral patterns of the aged 135-TMB SOA particles of Run 7 determined by FCM.

products from OH-initiated photooxidation of 135-TMB (Rickard et al., 2010; Sato et al., 2012; Huang et al., 2014). As depicted in Fig. 6, aldehydes can undergo subsequent attacked by OH radicals to form carboxylic acids (Sato et al., 2012; Huang et al., 2015). Added NH_3 may drive these gaseous organic acids to form particulate organic ammonium salts, such as ammonium methyl glyoxylate, ammonium 3,5-dimethylbenzoate shown in Fig. 5. These maybe responsible for the increased mass concentration of 135-TMB SOA when NH_3 is introduced as displayed in Fig. 1.

N-containing fragments are appeared in the mass pattern of Class 9–14 of aged 135-TMB SOA in the presence of NH_3 (Run 7) as shown in Fig. 5. Strong peaks belonging to the $C_xH_yN_n$ dominate the spectrum at m/z 28 (CH_2N^+), 41($C_2H_3N^+$) and 67($C_3H_3N_2^+$), demonstrating that imidazole species are formed in the aged 135-TMB SOA (Huang et al., 2017). In order to compare and validate the speculated aged products of imidazole compounds, 1H-imidazole, 4-methyl- 1H-imidazole, and 1H-imidazole-2-carboxaldehyde were dissolved, then atomized to generate aerosol particles and measured by ALTOFMS similar to two selected ammonium carboxylates as mentioned above. As shown in Supplementary Figs. S2–5, the mass spectra of 1H-imidazole, 4-methyl-1H-imidazole, and 1H-imidazole-2-carboxaldehyde measured by the ALTOFMS or downloaded from the NIST database contain the specific fragment peaks of imidazole compounds at m/z 28 (CH_2N^+), m/z 41 ($C_2H_3N^+$) and m/z 67 ($C_3H_3N_2^+$). After careful comparisons the mass spectra patterns of Class 9 to Class 14 with the average mass spectra of the standard chemicals shown in Supplementary Fig. S2 and the published spectra downloaded from the NIST database displayed in Supplementary Figs. S3–5, class 9 to class 14 could be tentatively identified to be imidazole compounds.

These results are in accordance with the previous studies which detected a notable increase in the fraction of organonitrogen compounds for aged α-pinene SOA (Flores et al., 2014) and m-xylene SOA with NH_3 (Liu et al., 2015). It is well known that methylglyxoxal is the major particulate α-dicarbonyls of product from the photoxidation of 135-TMB (Rickard et al., 2010; Sato et al., 2012; Huang et al., 2014). According to the experimental results of Liu et al. (2015) and Zhang et al. (2015), heterogeneous reactions of NH_3 with carbonyl compounds in SOA leading to the generation of imidazole products after the NH_3 uptake onto the SOA. As shown in Fig. 7, methylglyxoxal is protonated by hydrogen ion from organic acid products and hydrolyzed by diol product (1) and tetrol product (2) formation subsequently. Also, the protonated methylglyxoxal can be attacked by NH_3 followed by loss of H_2O and H^+ ion, producing diimine product (3), which then condenses (2) to generate 4-methyl-imidazole-2-acetaldehyde (4), 4-methyl-1H-imidazole (5) and they are derivatives (6)–(9) as depicted in Fig. 7.

3.4. Effect of NH_3 on the particulate products of aged 135-TMB SOA

To investigate how the NH_3 affect the ammonium carboxylates and imidazole products, the UV–Vis spectra of the aged 135-TMB SOA filter extracts for the Run 1 to Run 7 were measured, respectively. As shown in Fig. 8, the absorbance of 205 nm (corresponding to the content of ammonium carboxylates in aged 135-TMB SOA) increases as the added NH_3 increases from 0 to 20.3 ppm. However, the absorbance of 205 nm remained almost constant is noted as the concentration of NH_3 exceeds 8.0 ppm, while the absorption peak at 280 nm becomes discernable and its absorbance increases gradually and reaches a plateau after the concentration passes 16.0 ppm. Na et al. (2007) and Paciga et al. (2014) have observed the neutralization reaction between NH_3 and gaseous organic acids, leading to the generation of particle phase organic ammonium salts. As reactions of NH_3 with carbonyls are usually acid catalyzed (Zhang et al., 2015), Liu et al. (2015) suggested that the rates of gas phase reactions between NH_3 and carbonyls are exceedingly slow as a termolecular reaction would be necessary, and heterogeneous

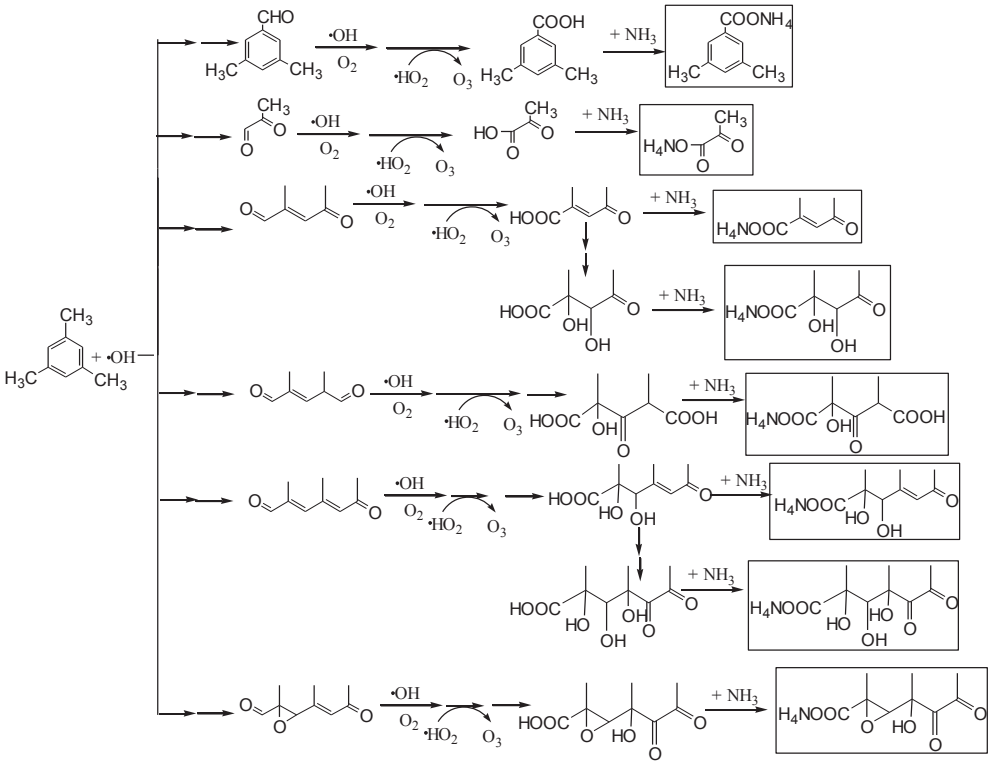


Fig. 6. Proposed aging mechanism leading to the formation of ammonium carboxylates.

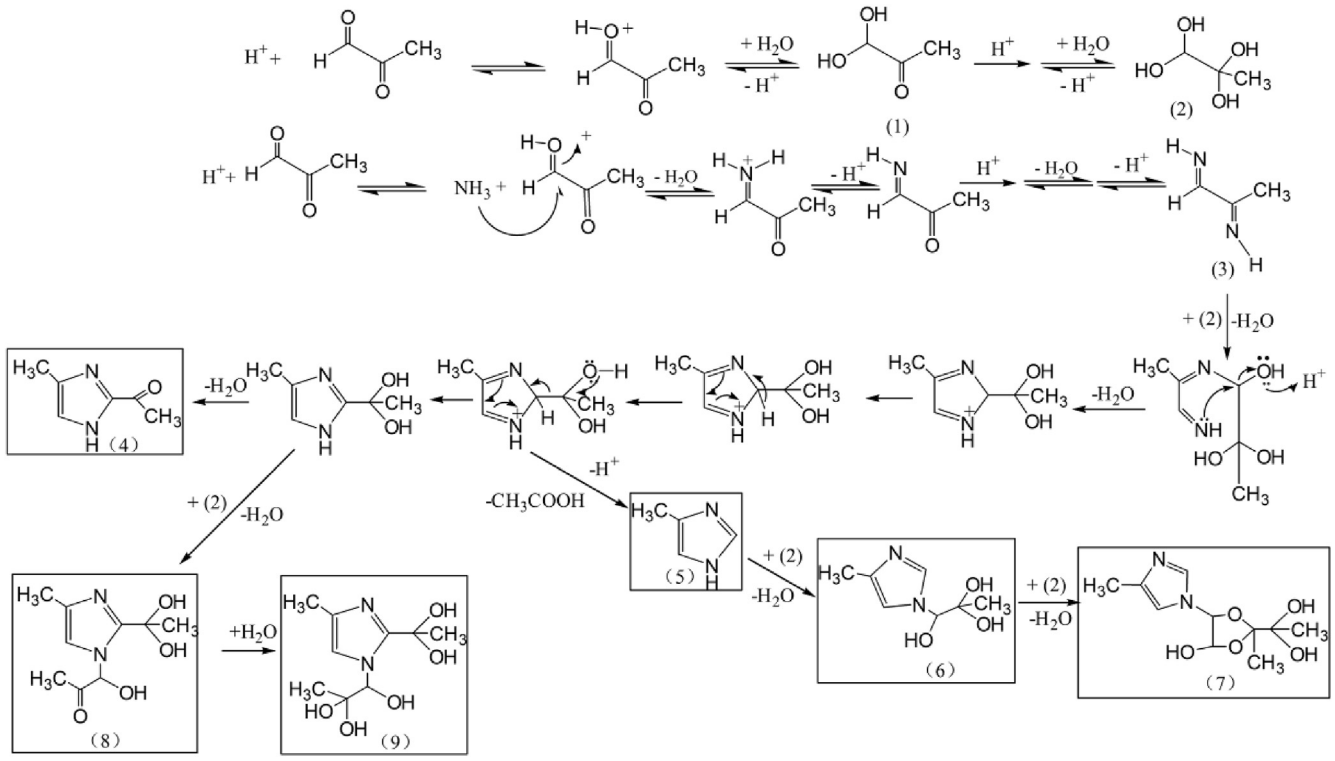


Fig. 7. Proposed aging mechanism leading to the formation of imidazole products.

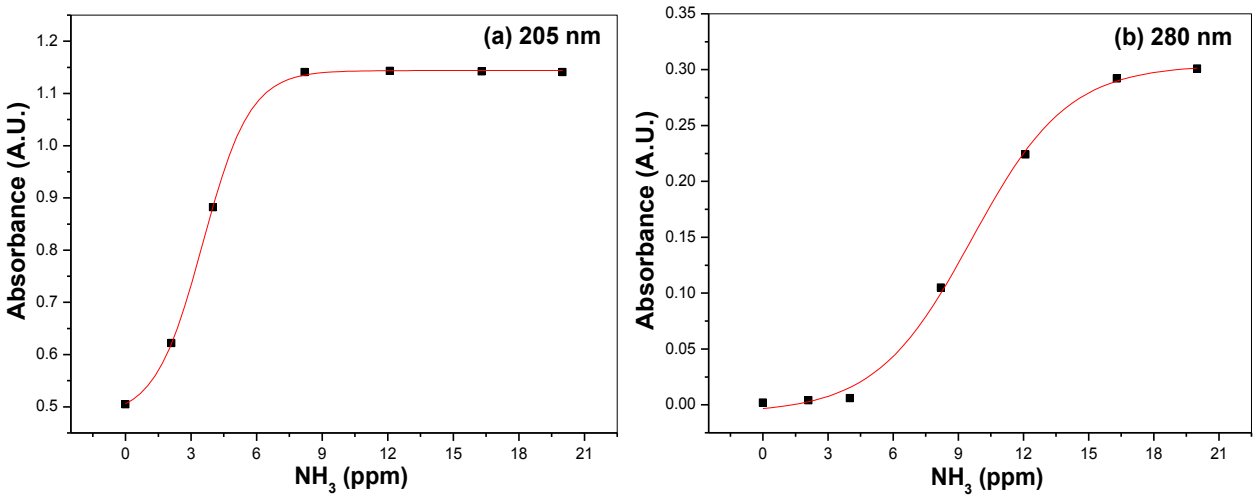


Fig. 8. The absorbance of (a) 205 nm and (b) 280 nm of filter extract of aged 135-TMB SOA in the presence of different concentration of NH_3.

reactions occur after NH_3 absorbed onto the SOA are contribute to the particulate imidazole products.

Based on the experimental results above, the effects of NH_3 on the ammonium carboxylates and imidazole products can be interpreted. Gas phase organic acids and carbonyls from the photooxidation of 135-TMB exposed to gaseous NH_3, acid-base neutralization reaction between gas-phase organic acids and NH_3 arises firstly. The resulting organic ammonium salts subsequent condensation leading to the increase of mass concentration of 135-TMB SOA. When the concentration of NH_3 increases to a certain value (8.0 ppm in this study), the gas phase organic acids were consumed completely, and the concentration of ammonium carboxylates (corresponding to the absorbance of 205 nm) remained nearly constant even if the concentration of NH_3 increased as observed in Run 4–7. Heterogeneous reactions occur via the uptake of NH_3 by 135-TMB SOA when the concentration of NH_3 exceeds 8.0 ppm, and facilitate the formation of imidazole products as mentioned above. It is no surprising that the concentration of imidazole products (corresponding to the absorbance of 280 nm) increases as the amount of the added NH_3 increases in Run 4–7. It is worth noting that no additional imidazole products generation is observed as the added NH_3 exceeds 16 ppm. This probably due to the particulate carbonyls present in this reaction, in terms of NH_3, have been consumed totally.

For further validate the effects of NH_3 on the formation and aging of 135-TMB SOA, Run 7 was repeated, and the formation SOA

particles after 6 h photooxidation were collected, extracted and measured by UV–Vis spectrophotometer as mentioned in Section 2.2. As shown in Supplementary Fig. S6, there is only the absorption band at 205 nm was found in the UV–Vis spectra, indicating that ammonium carboxylates are the major products in 135-TMB SOA particles after 6 h photooxidation. Before 6 h in this study, there were plenty of 135-TMB and OH radicals to generate gaseous organic acids and carbonyls (Fisseha et al., 2004; Sato et al., 2012; Huang et al., 2014). When these products exposed to NH_3, acid-base neutralization reaction between gaseous organic acids and NH_3 arises merely as mentioned above. The resulting organic ammonium salts subsequent condensation leading to the increase of mass concentration of 135-TMB SOA. The SOA increasing rate during first 6 h is proportional to the initial concentration of NH_3 as shown in Fig. 1, indicating that NH_3 has promotion effect on 135-TMB SOA formation via the reaction between gaseous organic acids and NH_3. Compared to the Supplementary Fig. S6, as displayed in Fig. 2, the additional absorption signal at 280 nm was emerged in the UV–Vis spectra of aged 135-TMB SOA particles of Run 7 after 24 h photoodation, demonstrating that new aging products of imidazole compounds via heterogeneous reactions of NH_3 with carbonyl functional groups in SOA were formation in the aged SOA particles. These results suggested that the gaseous organic acid reactions with NH_3 occur during first 6 h photooxidation, while carbonyls in SOA heterogeneous reaction with NH_3 during the 18 h aging period.

Compared to the experiments of Na et al. (2007) and Liu et al. (2015), the current work extended the concentration of NH_3 to 20 ppm, and the particulate products of aged 135-TMB SOA measured by ALTOFMS, UV–Vis and ATR-FTIR further strengthen the suggestion that NH_3 can react with gaseous organic acids generating condensable organic ammonium salts and enhancing SOA formation. Also, 4-methyl-imidazole-2-acetaldehyde, 4-methyl-1H-imidazole and they are derivatives which were formed form heterogeneous reactions between NH_3 and dialdehydes of SOA were newly detected. The results of this study also indicated that imidazole derivatives can be formed via the absorption of NH_3 by fresh SOA particles, in contrast to the experimental results of Bones et al. (2010) where organonitrogen products forms over several days. These would provide valuable information for SOA aging and new pathway for NH_3 deposition.

4. Conclusion

The current study was performed to examine the influence of NH_3 on the particulate products of aged 135-TMB SOA. The chemical constitutes of aged 135-TMB SOA in the presence of NH_3 were measured by UV–Vis, ATR-FTIR and ALTOFMS, respectively. The obtained results shown that NH_3 can react with gaseous organic acids generating condensable organic ammonium salts and enhancing SOA formation. 4-methyl-imidazole-2-acetaldehyde, 4-methyl-1H-imidazole and they are derivatives formed from heterogeneous reactions between NH_3 and dialdehydes of SOA were newly detected in this study. Imidazole compounds from this mechanism may be a potential source of the ambient particle associated nitrogen-containing organic compounds. Imidazole compounds have been regarded as an important class of brown carbon, which are considered to have a significant role in climate radiative forcing (Laskin et al., 2015).

It should be noted that relative humidity is another factor in the SOA formation and aging. Na et al. (2007) and Babar et al. (2017) have shown that initially present NH_3 enhanced aerosol yield in α-pinene/ozone reactions, regardless of the presence of water vapor in smog chamber and flow reactor, respectively. The extent of increase in SOA yield is higher in humid condition than that in the dry condition. They attributed this to that water vapor increases gaseous organic acid formation, which is subsequently converted into particle-phase organics by reacting with NH_3. As organic acids are the major products for the OH-initiated photoxidation of 135-TMB (Fisseha et al., 2004; Sato et al., 2012; Huang et al., 2015), similar results of the influence of relative humidity on SOA yield may be obtained in the 135-TMB/CH_3ONO/NO/NH_3 mixture system. The further experiments are needed to investigate the effect of relative humidity on the particulate products of NH_3-aged 135-TMB SOA and characterize the absorption properties of aged SOA thoroughly.

Acknowledgements

The authors thank Mr. Michael Nusbaum from Department of English, Xiamen University, Tan Kah Kee College for help with the English language. This work was supported by the National Natural Science Foundation of China (No. 41575118, 41305109, 21502086, 41575126), the Outstanding Youth Science Foundation of Fujian Province of China (No. 2015J06009) and the Natural Science Foundation of Fujian Province of China (No. 2015J05028, 2015J01062). Also, the authors express our gratitude to the referees for their valuable comments.

Appendix A. Supplementary data

Supplementary data related to this article can be found at http://dx.doi.org/10.1016/j.apr.2017.08.003.

References

Andreae, M.O., 2009. A new look at aging aerosols. Science 326, 1493–1494.
Andreae, M.O., Ramanathan, V., 2013. Climate's dark forcings. Science 340, 280–281.
Atkinson, R., Carter, W.P.L., Winer, A.M., 1981. An experimental protocol for the determination of OH radical rate constants with organics using methyl nitrite photolysis as an OH radical source. J. Air Pollut. Control Assoc. 31, 1090–1092.
Atkinson, R., Baulch, D.L., Cox, R.A., Crowley, J.N., Hampson, R.F., Hynes, R.G., Jenkin, M.E., Rossi, M.J., Troe, J., 2004. Evaluated kinetic and photochemical data for atmospheric chemistry: volume I – gas phase reactions of O_x, HO_x, NO_x and SO_x species. Atmos. Chem. Phys. 4, 1461–1738.
Babar, Z.B., Park, J.H., Lim, H.J., 2017. Influence of NH_3 on secondary organic aerosols from the ozonolysis and photooxidation of α-pinene in a flow reactor. Atmos. Environ. 164, 71–84.
Bones, D.L., Henricksen, D.K., Mang, S.A., Gonsior, M., Bateman, A.P., Nguyen, T.B., Cooper, W.J., Nizkorodov, S.A., 2010. Appearance of strong absorbers and fluorophores in limonene-O_3 secondary organic aerosol due to NH_4^+-mediated chemical aging over long time scales. J. Geophys. Res. Atmos. 115 (D05203), 1–14.
Carlton, A.G., Turpin, B.J., Altieri, K.E., Seitzinger, S., Reff, A., Lim, H.J., Ervens, B., 2007. Atmospheric oxalic acid and SOA production from glyoxal:Results of aqueous photooxidation experiments. Atmos. Environ. 41, 7588–7602.
Chang, J.L., Thompson, J.E., 2010. Characterization of colored products formed during irradiation of aqueous solutions containing H_2O_2 and phenolic compounds. Atmos. Environ. 44, 541–551.
Fisseha, R., Dommen, J., Sax, M., Paulsen, D., Kalberer, M., Maurer, R., Hö1fler, F., Weingartner, E., Baltensperger, U., 2004. Identification of organic acids in secondary organic aerosol and the corresponding gas phase from chamber experiments. Anal. Chem. 76, 6535–6540.
Flores, J.M., Washenfelder, R.A., Adler, G., Lee, H.J., Segev, L., Laskin, J., Laskin, A., Nizkorodov, S.A., Brown, S.S., Rudich, Y., 2014. Complex refractive indices in the near- ultraviolet spectral region of biogenic secondary organic aerosol aged with ammonia. Phys. Chem. Chem. Phys. 16, 10629–10642.
Gentner, D.R., Jathar, S.H., Gordon, T.D., Bahreini, R., Day, D.A., Haddad, I.E., Hayes, P.L., Pieber, S.M., Platt, S.M., Gouw, J., Goldstein, A.H., Harley, R.A., Jimenez, J.L., Prévôt, A.S.H., Robinson, A.L., 2017. Review of urban secondary organic aerosol formation from gasoline and diesel motor vehicle emissions. Environ. Sci. Technol. 51, 1074–1093.
George, I.J., Abbatt, J.P.D., 2010. Chemical evolution of secondary organic aerosol from OH-initiated heterogeneous oxidation. Atmos. Chem. Phys. 10, 5551–5563.
Huang, M.Q., Hao, L.Q., Gu, X.J., Hu, C.J., Zhao, W.X., Wang, Z.Y., Fang, L., Zhang, W.J., 2013. Effects of inorganic seed aerosols on the growth and chemical composition of secondary organic aerosol formed from OH-initiated oxidation of toluene. J. Atmos. Chem. 70, 151–164.
Huang, M.Q., Hu, C.J., Guo, X.Y., Gu, X.J., Zhao, W.X., Wang, Z.Y., Fang, L., Zhang, W.J.,

2014. Chemical composition of gas and particle-phase products of OH–initiated oxidation of 1,3,5-trimethylbenzene. Atmos. Pollut. Res. 5, 73–78.
Huang, M.Q., Lin, Y.H., Huang, X.Y., Liu, X.Q., Guo, X.Y., Hu, C.J., Zhao, W.X., Gu, X.J., Fang, L., Zhang, W.J., 2015. Experimental study of particulate products for aging of 135-trimethyl benzene secondary organic aerosol. Atmos. Pollut. Res. 6, 209–219.
Huang, M.Q., Hao, L.Q., Cai, S.Y., Gu, X.J., Zhang, W.X., Hu, C.J., Wang, Z.Y., Fang, L., Zhang, W.J., 2017. Effects of inorganic seed aerosols on the particulate products of aged 1,3,5- trimethylbenzene secondary organic aerosol. Atmos. Environ. 152, 490–502.
Kampf, C.J., Jakob, R., Hoffmann, T., 2012. Identification and characterization of aging products in the glyoxal/ammonium sulfate system - implications for light-absorbing material in atmospheric aerosols. Atmos. Chem. Phys. 12, 6323–6333.
Kroll, J.H., Smith, J.D., Che, D.L., Kessler, S.H., Worsnop, D.R., Wilson, K.R., 2009. Measurement of fragmentation and functionalization pathways in the heterogeneous oxidation of oxidized organic aerosol. Phys. Chem. Chem. Phys. 11, 8005–8014.
Laskin, A., Laskin, J., Nizkorodov, S.A., 2015. Chemistry of atmospheric brown carbon. Chem. Rev. 115, 4335–4382.
Lee, A.K.Y., Zhao, R., Li, R., Liggio, J., Li, S.M., Abbatt, P.D., 2013. Formation of light absorbing organo-nitrogen species from evaporation of droplets containing glyoxal and ammonium sulfate. Environ. Sci. Technol. 47, 12819–12826.
Li, L.J., Tang, P., Nakao, S.S., Kacarab, M., Cocker III, D.R., 2016. Novel approach for evaluating secondary organic aerosol from aromatic hydrocarbons: unified method for predicting aerosol composition and formation. Environ. Sci. Technol. 50, 6249–6256.
Li, K., Wang, W.G., Ge, M.F., Li, J.J., Wang, D., 2014. Optical properties of secondary organic aerosols generated by photooxidation of aromatic hydrocarbons. Sci. Rep. 4, 1–9.
Lin, P., Liu, J.M., Shilling, J.E., Kathmann, S.M., Laskin, J., Laskin, A., 2015. Molecular characterization of brown carbon (BrC) chromophores in secondary organic aerosol generated from photo-oxidation of toluene. Phys. Chem. Chem. Phys. 17, 23312–23325.
Liu, Y., Liggio, J., Staebler, R., Li, S.M., 2015. Reactive uptake of ammonia to secondary organic aerosols: kinetics of organonitrogen formation. Atmos. Chem. Phys. 15, 13569–13584.
Maxut, A., Nozière, B., Fenet, B., Mechakra, H., 2015. Formation mechanism and yield of small imidazoles from reactions of glyoxal with NH_4^+ in water at neutral pH. Phys. Chem. Chem. Phys. 17, 20416–20424.
Na, K., Song, C., Switze, R.C., Cocker III, D.R., 2007. Effect of ammonia on secondary organic aerosol formation from α-pinene ozonolysis in dry and humid conditions. Environ. Sci. Technol. 41, 6096–6102.
Nakayama, T., Sato, K., Matsumi, Y., Imamura, T., Yamazaki, A., Uchiyama, A., 2013. Wavelength and NO_x dependent complex refractive index of SOAs generated from the photooxidation of toluene. Atmos. Chem. Phys. 13, 531–545.
Paciga, A.L., Riipinen, I., Pandis, S.N., 2014. Effect of ammonia on the volatility of organic diacids. Environ. Sci. Technol. 48, 13769–13775.
Paulot, F., Jacob, D.J., Pinder, R.W., Bash, J.O., Travis, K., Henze, D.K., 2014. Ammonia emissions in the United States, European Union, and China derived by high-resolution inversion of ammonium wet deposition data: interpretation with a new agricultural emissions inventory (MASAGE_NH_3). J. Geophys. Res. Atmos. 119, 4343–4364.
Rickard, A.R., Wyche, K.P., Metzger, A., Monks, P.S., Ellis, A.M., Dommen, J., Baltensperger, U., Jenkin, M.E., Pilling, M.J., 2010. Gas phase precursors to anthropogenic secondary organic aerosol: using the master chemical mechanism to probe detailed observations of 1,3,5- trimethylbenzene photo-oxidation. Atmos. Environ. 44, 5423–5433.
Rudich, Y., Donahue, N.M., Mentel, T.F., 2007. Aging of organic aerosol: bridging the gap between laboratory and field studies. Annu. Rev. Phys. Chem. 58, 321–352.
Sato, K., Takami, A., Kato, Y., Seta, T., Fujitani, Y., Hikida, T., Shimono, A., Imamura, T., 2012. AMS and LC/MS analyses of SOA from the photooxidation of benzene and 1,3,5-trimethyl benzene in the presence of NO_x: effects of chemical structure on SOA aging. Atmos. Chem. Phys. 12, 4667–4682.
Silva, P.J., Prather, K.A., 2000. Interpretation of mass spectra from organic compounds in aerosol time-of-flight mass spectrometry. Anal. Chem. 72, 3553–3562.
Sun, K., Tao, L., Miller, D.J., Pan, D., Golston, L.M., Zondlo, M.A., Griffin, R.J., Wallace, H.W., Leong, Y.J., Yang, M.M., Zhang, Y., Mauzerall, D.L., Zhu, T., 2017. Vehicle emissions as an important urban ammonia source in the United States and China. Environ. Sci. Technol. 51, 2472–2481.
Tang, M.J., Alexander, J.M., Kwon, D., Estillore, A.D., Laskina, O., Young, M.A., Kleiber, P.D., Grassian, V.H., 2016. Optical and physicochemical properties of brown carbon aerosol: light scattering, FTIR extinction spectroscopy, and hygroscopic growth. J. Phys. Chem. A 120, 4155–4166.
Updyke, K.M., Nguyen, T.B., Nizkorodov, S.A., 2012. Formation of brown carbon via reactions of ammonia with secondary organic aerosols from biogenic and anthropogenic precursors. Atmos. Environ. 63, 22–31.
Zhang, R., Wang, G., Guo, S., Zamora, M.L., Ying, Q., Lin, Y., Wang, W.G., Hu, M., Wang, Y., 2015. Formation of urban fine particulate matter. Chem. Rev. 115, 3803–3855.
Ziemann, P.J., Atkinson, R., 2012. Kinetics, products, and mechanisms of secondary organic aerosol formation. Chem. Soc. Rev. 41, 6582–6605.